



Cite this: *Integr. Biol.*, 2017, 9, 519

## Microfluidic analysis of red blood cell deformability as a means to assess hemin-induced oxidative stress resulting from *Plasmodium falciparum* intraerythrocytic parasitism

Kerryn Matthews,<sup>a</sup> Simon P. Duffy,<sup>a</sup> Marie-Eve Myrand-Lapierre,<sup>a</sup> Richard R. Ang,<sup>a</sup> Li Li,<sup>bd</sup> Mark D. Scott<sup>bcd</sup> and Hongshen Ma<sup>id\*abcef</sup>

Hemolytic anemia is one of the hallmarks of malaria and leads to an increase in oxidized heme (hemin) within the plasma of infected individuals. While scavenger proteins sequester much of the circulating heme, it has been hypothesized that extracellular heme may play a central role in malaria pathogenesis. We have previously developed the multiplex fluidic plunger (MFP) device for the measurement of red blood cell (RBC) deformability. Here, we demonstrate that the measurement of changes in RBC deformability is a sensitive method for inferring heme-induced oxidative stress. We further show that extracellular heme concentration correlates closely with changes in RBC deformability and we confirm that this biophysical change correlates with other indicators of cell stress. Finally, we show that reduced erythrocyte deformability corresponds with both erythrophagocytosis and RBC osmotic fragility. The MFP microfluidic device presents a simple and potentially inexpensive alternative to existing methods for measuring hemolytic cell stress that could ultimately be used to perform clinical assessment of disease progression in severe malaria.

Received 28th February 2017,  
Accepted 12th May 2017

DOI: 10.1039/c7ib00039a

rsc.li/integrative-biology

### Insight, innovation, integration

During malaria infection, red blood cells experience heme-induced oxidative stress, resulting in cell lysis and the development of hemolytic anemia in patients. This study applies a recently developed microfluidic technology to assess the deformability of individual red blood cells. The results show that red blood cell deformability provides a sensitive measure of hemolytic cell stress closely correlating to both erythrophagocytosis and osmotic fragility. Consequently, this approach provides a simple and sensitive method for measuring hemolytic cell stress that could ultimately be used to perform clinical assessment of disease progression in severe malaria.

## Introduction

Malaria is an infectious disease transmitted by mosquito-borne parasites (*Plasmodium* spp.) and is the leading cause of death and disease in developing nations. Specifically, malaria has been attributed to an estimated 198 million infections and

584 000 deaths, annually.<sup>1</sup> Central to the pathogenesis of malaria is the proteolysis of hemoglobin to heme, which is stored in the parasite digestive vacuole as inert hemozoin.<sup>2</sup> However, intraerythrocytic parasitism ultimately contributes to hemolysis and the subsequent release of cytotoxic hemoglobin and heme. While circulating heme is normally sequestered by scavenger proteins and delivered to cells for detoxification by heme-oxygenase, this heme trapping mechanism can be easily overwhelmed. Such an excess of heme contributes to severe damage to the vascular tissue as well as the liver, kidney and spleen due to the oxidative effects of heme metabolites,<sup>3</sup> as well as a hyperactive immune response.<sup>4</sup> Extracellular heme also has a potent effect on bystander red blood cells (RBCs), where it induces cytoskeletal cross-linking<sup>5</sup> and lipid peroxidation.<sup>6,7</sup> These damaged RBCs lose their ability to deform and are subsequently sequestered from circulation<sup>8</sup> via erythrophagocytosis,<sup>9</sup> resulting in hemolytic anemia.

<sup>a</sup> Department of Mechanical Engineering, University of British Columbia, 2054-6250 Applied Science Lane, Vancouver, BC, V6T 1Z4, Canada. E-mail: hongma@mech.ubc.ca

<sup>b</sup> Centre for Blood Research, University of British Columbia, Vancouver, BC, Canada

<sup>c</sup> Department of Pathology and Laboratory Medicine, University of British Columbia, Vancouver, BC, Canada

<sup>d</sup> Canadian Blood Services, University of British Columbia, Vancouver, BC, Canada

<sup>e</sup> Department of Urologic Science, University of British Columbia, Vancouver, BC, Canada

<sup>f</sup> Vancouver Prostate Centre, Vancouver General Hospital, Vancouver, BC, Canada

Given the central role of heme in the pathology of malaria, monitoring hemolytic stress of both parasitized and bystander RBCs could provide indication of disease progression. Since direct analysis of extracellular heme is challenging, due to its intercalation within lipid membranes, oxidative stress is typically inferred instead by measurement of reactive oxygen species (ROS) or phosphatidylserine (PS) externalization.<sup>8,9</sup> However, the non-specific nature and short half-life of ROS confounds their direct analysis<sup>10</sup> and assessment of both ROS and PS externalization requires sophisticated instrumentation that is not always available in resource-poor regions, where malaria is endemic. In contrast to short lived ROS, the associated cytoskeletal cross-linking and lipid peroxidation contribute to a long-lasting decrease in RBC deformability, and measurement of RBC deformability could therefore provide an alternative means to evaluate hemolytic oxidative stress in RBCs.

RBC deformability has been investigated as an indicator for severe hemolytic malaria,<sup>11–13</sup> and for assessment of malaria drug efficacy<sup>14–16</sup> but cell deformability has proven difficult to measure. For example, ektacytometry has been applied to clinical assessment of RBC deformability but this method only measures the mean cell deformability of the RBC population and cannot be used to discriminate single cells under oxidative stress, when they are diluted among the unaffected population of normal RBCs in circulation.<sup>17–23</sup> Single cell analytical methods also exist, such as optical tweezers<sup>24</sup> or microfluidic systems that employ wedging in tapered constrictions,<sup>25,26</sup> quantification of blood flow,<sup>27,28</sup> elongation *via* fluid shear stress,<sup>29,30</sup> transit pressure through microscale constrictions,<sup>31</sup> and transit time through microscale constrictions.<sup>32,33</sup> However, despite this diverse array of analytical approaches, no single method has yet delivered both the sensitivity and sample throughput needed for the clinical assessment of malaria.

To address the need for a rapid and sensitive clinical RBC deformability assay, we previously developed the multiplexed fluidic plunger (MFP).<sup>14</sup> This mechanism involves the deformation of RBCs through microscale funnels within a microchannel. The pressure required for RBCs to transit through the microstructures correlates directly with the deformability of the cell. To allow for the measurement of multiple cells simultaneously, we have arranged the microchannels in parallel. Here, we specifically apply this technology to the assessment of biophysical changes in RBCs following hemin-induced oxidative stress. In contrast with short-lived ROS, changes in RBC deformability represent a sustained and robust indicator of oxidative stress, and this rapid single cell analysis provides a practical approach for the clinical assessment of hemolytic oxidative stress.

## Experimental

### Blood samples and preparation

Whole blood was obtained from nine healthy donors between the ages of 22 and 40, after informed consent. The study was approved by and carried out in strict accordance with the guidelines and regulations of the University of British Columbia's Clinical

Research Ethics Board. A total of 5  $\mu$ l of blood was diluted in 1 ml of Hanks Balanced Salt Solution (HBSS, Gibco, Grand Island, NY) supplemented with 5 mM glucose (Sigma-Aldrich, St. Louis, MO). Hemin (Protoporphyrin IX, Sigma-Aldrich, St. Louis, MO) dissolved to 2 mM in 20 mM NaOH (Sigma-Aldrich, St. Louis, MO) and RBCs were incubated in 0, 25, 50 and 100  $\mu$ M at 37 °C, 5% CO<sub>2</sub> for 24 hours. After incubation, samples were washed 3 times in Phosphate Buffered Saline (PBS, Gibco, Grand Island, NY) by centrifugation at 250g for 5 minutes, after which an aliquot was used for flow cytometry and the remainder was resuspended in assay buffer, which consisted of PBS with 0.2% Pluronic F-127 (Sigma-Aldrich, St. Louis, MO), for deformability measurements.

### Device fabrication and procedure for erythrocyte deformability measurements

The multiplex fluidic plunger device was fabricated and operated as described by Myrand-Lapierre, *et al.*<sup>14</sup> The device consists of 34 micro-constrictions (Fig. 1), each with a pore size of  $\sim$ 2.4  $\mu$ m and a height of  $\sim$ 3.7  $\mu$ m (Fig. 1B). Briefly, a low pressure (0.3–1.0 mbar) was used to load RBCs into the device through the cell inlet (Fig. 1C and D). The applied pressure was sufficient to cause RBCs to occupy but not to transit the micro-constrictions. We have previously observed that all cells experience equal deformation pressure and that unoccupied microconstrictions do not affect deformability measurement,<sup>14</sup> but for ease of analysis the infusion process was continued until the majority of constrictions were occupied. The pressure was increased in increments of 1.0 mbar per second until the RBCs passed through the constrictions. In cases where the RBCs remained in the constrictions, the cells were either flushed through the constriction by an applied pressure up to 1000 mbar or detached by reverse flow. After the microconstrictions were clear, the device was washed with buffer and more RBCs were infused until at least 100 cell deformability measurements could be obtained. In this way, a single device was used for each donor and both cell infusion and measurement of threshold deformation pressure for >100 cells could be accomplished within 10 minutes. This deformation pressure was recorded by video microscopy, using automated video software (Fig. 2A), and this measurement was used to extrapolate the precise constriction transit pressure for each RBC (Fig. 2B). The same device was used to assess all 4 hemin concentrations (0, 25, 50 and 100  $\mu$ M) for each donor and was washed out with assay buffer between samples. Using the same device minimizes any variability in RBC deformability that may exist within samples from the same donor. To diminish the variability in RBC deformability that exists between donors,<sup>34</sup> all results were normalized to control data for each donor and the acquired videos were further analyzed for RBCs classified as abnormal, due to evidence of vesiculation, echinocytosis, Heinz body formation or other membrane changes from normal RBCs (Fig. 2C).

### Flow cytometry

DCF-DA staining was performed as previously described.<sup>35</sup> A 1  $\mu$ l aliquot of whole blood was diluted in 1 ml PBS and stained with 20  $\mu$ M 2',7'-dichlorofluorescein diacetate (DCF-DA, Sigma-Aldrich, St. Louis, MO) for 30 minutes at 37 °C, 5% CO<sub>2</sub> in the dark.

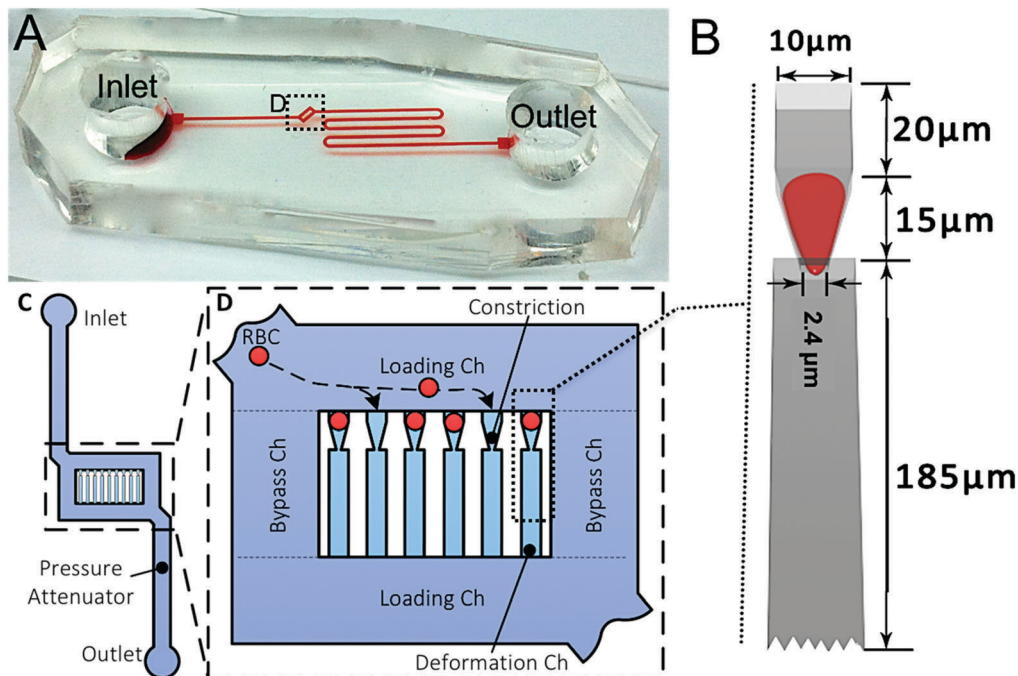


**Fig. 1** The multiplexed fluidic plunger. The MFP device was used to measure the deformability of RBCs treated with hemin. (A) Photograph of the MFP microfluidic device on a  $25 \times 75$  mm glass slide. (B) Magnified 3D model of one of the deformation channels, showing its dimensions and a RBC in planar configuration. (C) 2D model of the device showing a (D) magnified view of the rectangular shaped microchannel array with 2 loading channels and 2 bypass channels. The 34-channel device is represented here with only 6 channels for the purpose of illustration.

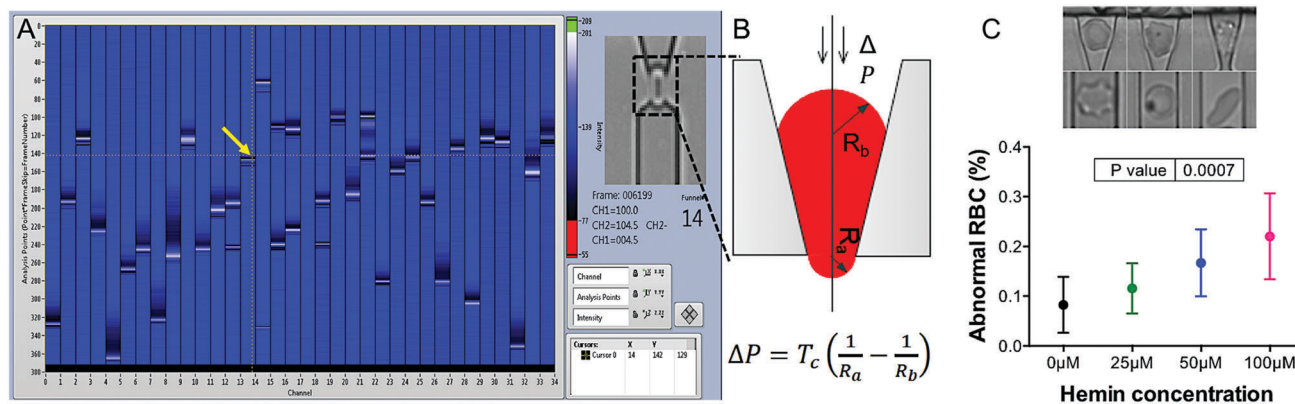


**Fig. 2** RBC deformability measurements and analysis using video recorded from each experiment performed using the MFP device. (A) Software designed specifically for MFP analysis was used to record the exact pressure that the RBC of interest (yellow arrow, and right inset) transited the constriction. (B) The pressure was then used to calculate the cortical tension ( $T_c$ ) for each RBC at the critical point of transit through the constriction using the Laplace Law calculation as shown. (C) RBCs showing vesiculation, echinocytosis or other abnormal morphology were counted in each experiment. Proportions of abnormal RBCs increased with increasing hemin concentration.

After incubation, RBCs were washed 3 times with PBS and incubated in 0, 25, 50 and 100  $\mu\text{M}$  hemin, in HBSS with 5 mM glucose, for 24 hours at 37  $^\circ\text{C}$ , 5%  $\text{CO}_2$ . The RBCs were further washed 3 times in PBS and mean fluorescence intensity was measured using a FACSCalibur (BD Biosciences).

Annexin-V staining was performed on hemin-stimulated RBCs, suspended to  $10^6$  cells per  $\mu\text{l}$ . A 1  $\mu\text{l}$  aliquot of hemin-stimulated RBCs was diluted in 200  $\mu\text{l}$  of  $1\times$  Binding Buffer and Annexin-V-FITC antibody (Clontech Laboratories Inc, Mountain View, CA) for 15 minutes in the dark at room temperature and

acquired on a FACSCalibur (BD Biosciences). Acquisition settings were set to a logarithmic scale for RBCs and analyzed with FlowJo (Trestar).

#### Effect of hemin challenge of human RBC on monocyte recognition and osmotic fragility

RBCs were treated with 0, 25, 50 or 100  $\mu\text{M}$  hemin for 60 minutes at 37  $^\circ\text{C}$ . Subsequent to hemin challenge, the cells were washed 3 times in PBS prior to analysis *via* the monocyte monolayer assay (MMA) and osmotic fragility assay. Hemin treated RBCs were

overlaid on the monocyte monolayer at 37 °C for 60 minutes. Concurrent with the hemin treated cells, negative and positive control samples were also examined. The negative control consisted of RhD<sup>+</sup> RBC incubated with buffer alone while the positive control consisted of RhD<sup>+</sup> RBC opsonized with a commercial anti-RhD antibody (PRho(D) Immune Globulin (Human) RhoGAM Ultra-Filtered PLUS; Ortho Clinical Diagnostics). Both negative and positive controls were similarly washed (3 times in PBS) and overlaid on a monocyte monolayer at 37 °C for 60 minutes and then counted as previously described.<sup>36–40</sup>

The structural stability of the control and hemin-treated RBC was examined *via* osmotic fragility studies as previously described.<sup>41,42</sup> Samples were resuspended to 10% hematocrit and 100 µl of control or hemin treated RBC were added to microcentrifuge tubes containing 1 ml of the saline concentrations. Samples were mixed by inversion and processed immediately. Total and supernatant hemoglobin concentrations were determined at the indicated time points by Drabkin's reagent to determine percent lysis.

### ***P. falciparum* cell culture supernatant stimulation and hemin measurement**

*P. falciparum*-infected RBCs were cultured between 2–3% parasitemia, as previously described<sup>43</sup> and mixed stage infected RBCs were centrifuged at 600g for 10 min. Supernatant was stored at –20 °C before it was assayed for free hemin using the Hemin Assay Kit (Sigma-Aldrich, St. Louis, MO). Whole blood from 3 donors was incubated with 100 µl of supernatant (final hematocrit of 10%) for 24 hours at 37 °C, 5% CO<sub>2</sub>. Whole blood in complete malaria media was used as the control, to which the supernatant treated samples were normalized. RBCs were washed 3 times in PBS by centrifugation at 250g for 5 minutes and resuspended in assay buffer for deformability measurements.

### **Statistical analysis**

Deformability results were analyzed using Graphpad Prism v6. Mean with Standard Deviation (SD) were plotted for individual donor and combined deformability results unless otherwise stated. Student *t*-test and ANOVA was used to determine statistical differences between results that were normally distributed, while Mann–Whitney and Kruskal–Wallis test were used for results that were not parametric. Gaussian curves of the distributions were plotted using Histograms with a Bin separation of 1.

## **Results**

### **Analysis of RBC deformability by multiplex fluidic plunger (MFP)**

Clinical assessment of hemolytic stress through the analysis of ROS has been hindered by the short-lived nature of these cellular metabolites.<sup>44</sup> While RBC deformability has long been proposed as an alternative biomarker for hemolytic stress, the use of this biophysical marker has been severely hindered by a lack of rapid and sensitive deformability measurement methods. We previously developed the MFP device to specifically enable

rapid evaluation of RBC deformability.<sup>14,34</sup> Briefly, whole blood is flowed through the inlet of the device, wherein individual RBCs align within parallel tapered deformation channels (Fig. 1). Precisely controlled pressure is applied to the microchannels and the minimum pressure required for each RBC to transit through the constriction is recorded in order to determine the deformability of the cell.

### **Hemin induces a concentration dependent loss in RBC deformability**

To assess whether RBC deformability could be employed as a robust marker for hemin-induced oxidative stress, we measured the cell deformability of hemin-induced RBCs. These cells were incubated over a range of hemin concentrations and the threshold pressure for transit of RBCs through the MFP microchannel was measured. This process involves gradually increasing the applied pressure and the use of digital microscopy to record cell transit and the corresponding deformation pressure for each cell (Fig. 2A). The microchannel taper structure allows for the calculation of RBC cortical tension, using Laplace's Law<sup>45,46</sup> (Fig. 2B) to provide a measure of the deformability of each RBC. Thirty-four microchannels are arranged in parallel, within the field of view, to allow for the simultaneous characterization of these cells.

Using parallel characterization of RBCs, at least 100 individual cells were analyzed for each hemin concentration. Prior to the deformation of RBCs through the funnel microstructure, we enumerated the number of cells displaying abnormal morphology, such as those that are indicative of cell vesiculation, echinocytosis, Heinz body formation or other membrane aberrations (Fig. 2C). This analysis revealed a dose dependent correlation between hemin concentration and the appearance of abnormal RBC morphology (ANOVA,  $p = 0.0007$ ). Irrespective of hemin concentration, the overall fraction of morphologically abnormal RBCs did not exceed a mean of 0.2% ( $n = 5$  RBCs at 100 µM hemin). To eliminate potential bias, these cells were excluded from subsequent deformability measurements.

We evaluated three criteria for assessing the effects of hemin-induced oxidative stress on RBCs. First, we examined the oxidative effects of hemin using flow cytometry and showed that the RBCs displayed a significant dose-dependent increase in ROS, as indicated from membrane-permeable 2',7'-dichlorofluorescein diacetate (DCF-DA) staining (Fig. 3A, Kruskal–Wallis, ANOVA  $p < 0.0001$ ). Next, we correlated RBC cortical tension with hemin concentration using the MFP device. We observed a significant dose dependent increase in cortical tension of hemin treated RBCs, relative to untreated controls (Fig. 3B, Kruskal–Wallis ANOVA  $p = 0.0011$ ). Finally, based on the observation that a subpopulation of RBCs frequently failed to transit the microfluidic microstructures, we then assessed whether the frequency of RBC retention in the microstructures was related to hemin concentration. The frequency of RBC retention was consistent with cortical tension in that there was a significant correlation with hemin concentration (Fig. 3C, Kruskal–Wallis ANOVA  $p = 0.0009$ ).

We also leveraged the capacity for single cell analysis to enable specific assessment of RBC subpopulations. To assess



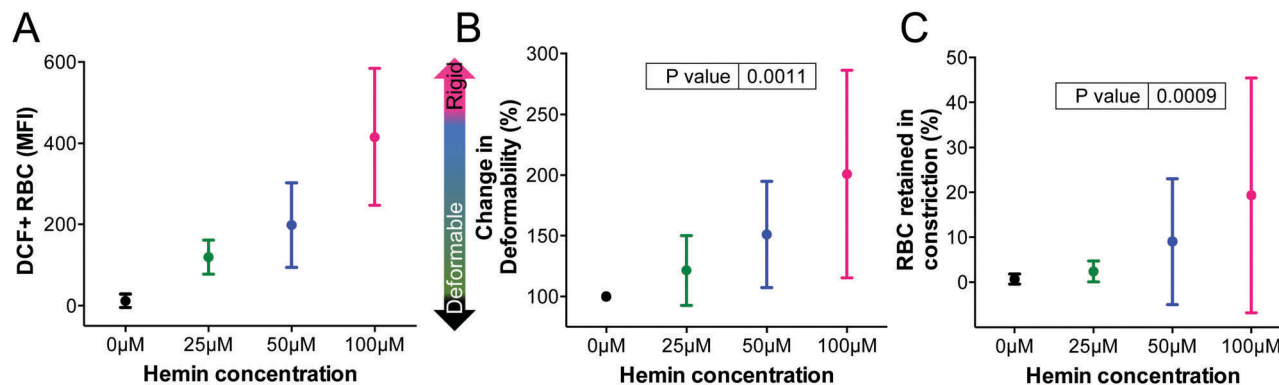


Fig. 3 Hemin induces oxidative stress which causes an increase in the rigidity of RBCs. (A) Flow cytometry of cells stained with 2',7'-dichlorofluorescein diacetate (DCF-DA) was used to assess mean fluorescent intensity (MFI) as a measure of oxidative stress. A significant dose-dependent correlation was observed between hemin concentration and MFI (mean  $\pm$  SD, ANOVA,  $p < 0.0001$ ). (B) The percent change in deformability (increase in cortical tension), relative to the untreated control (Kruskal–Wallis ANOVA  $p = 0.0011$ ), and (C) the proportion of RBCs that fail to transit the device microstructures both significantly correlate with hemin concentration, based on Kruskal–Wallis ANOVA ( $p = 0.0009$ ).

only those cells most sensitive to hemin oxidative stress, we restricted analysis to the least deformable 10% of RBCs from each experiment<sup>14</sup> (Fig. 4A). While overlap in RBC deformability is still observed in this distribution, the cells show less variation in relative cortical tension and there is a more significant correlation between the deformability of these cells and hemin concentration (Fig. 4B, Kruskal–Wallis ANOVA  $p < 0.0001$ ).

#### Hemin-mediated reduction in deformability corresponds with the externalization of phosphatidylserine (PS) on the cell surface

Given that PS externalization is emerging as a valuable biomarker for oxidative cell stress, during malaria infection, we evaluated the correspondence between changes in RBC deformability and the externalization of PS. PS externalization may occur by gradual translocation of PS to the outer leaflet of the cell membrane, as a consequence of cell senescence or eryptosis, which is the suicidal death of RBCs that involves cell shrinking and cell surface blebbing.<sup>47</sup> Oxidative stress drives the externalization of PS in bystander RBCs<sup>48</sup> and the accumulation of PS on the outer surface of the cell has been observed to increase over the course of both lethal and non-lethal *P. yoelii* infection in mice.<sup>49</sup> While it

represents a potentially valuable marker for monitoring the progression of malaria, assessment of PS externalization requires sophisticated flow cytometry instrumentation. Conversely, the MFP deformability measurement device can be integrated with a standard microscope that is fitted with a digital camera. Furthermore, the complementary software is designed to enable rapid measurement of cell deformability with minimal technical expertise.

Consistent with previous reports that PS externalization arises during oxidative stress, we observed that incubation of the cells with 100  $\mu$ M hemin resulted in a measurable increase in PS externalization, as determined by staining with FITC-conjugated Annexin-V (Fig. 5A). There was a significant increase in Annexin-V staining when RBCs were treated with 100  $\mu$ M hemin ( $p = 0.0075$ ). Since both biophysical changes in RBC and PS externalization are thought to be driven by oxidative stress it is not surprising that there was a positive correlation between mean cortical tension of each sample and the proportion of Annexin-V stained cells (Fig. 5C). However, the correlation between these parameters was only moderate ( $r = 0.6289$ ,  $p < 0.0001$ ), and this likely reflects the fact that cortical tension changes in a linear fashion (Fig. 4A), in response to oxidative stress, while PS

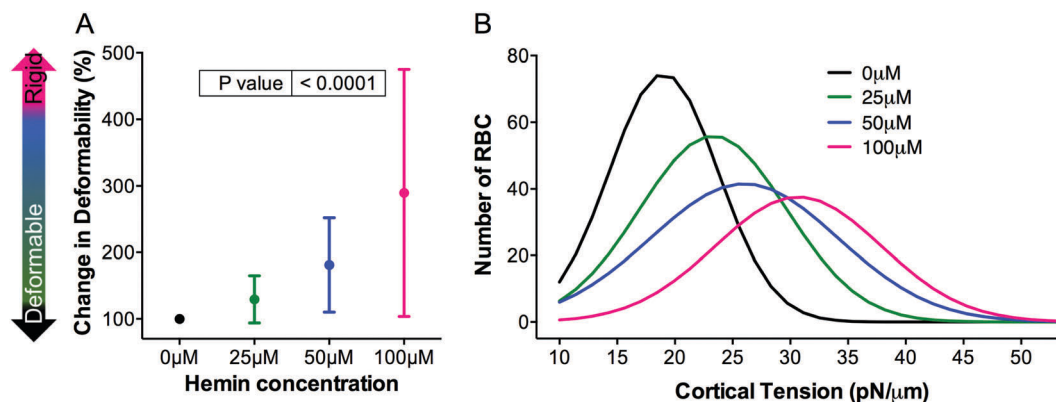
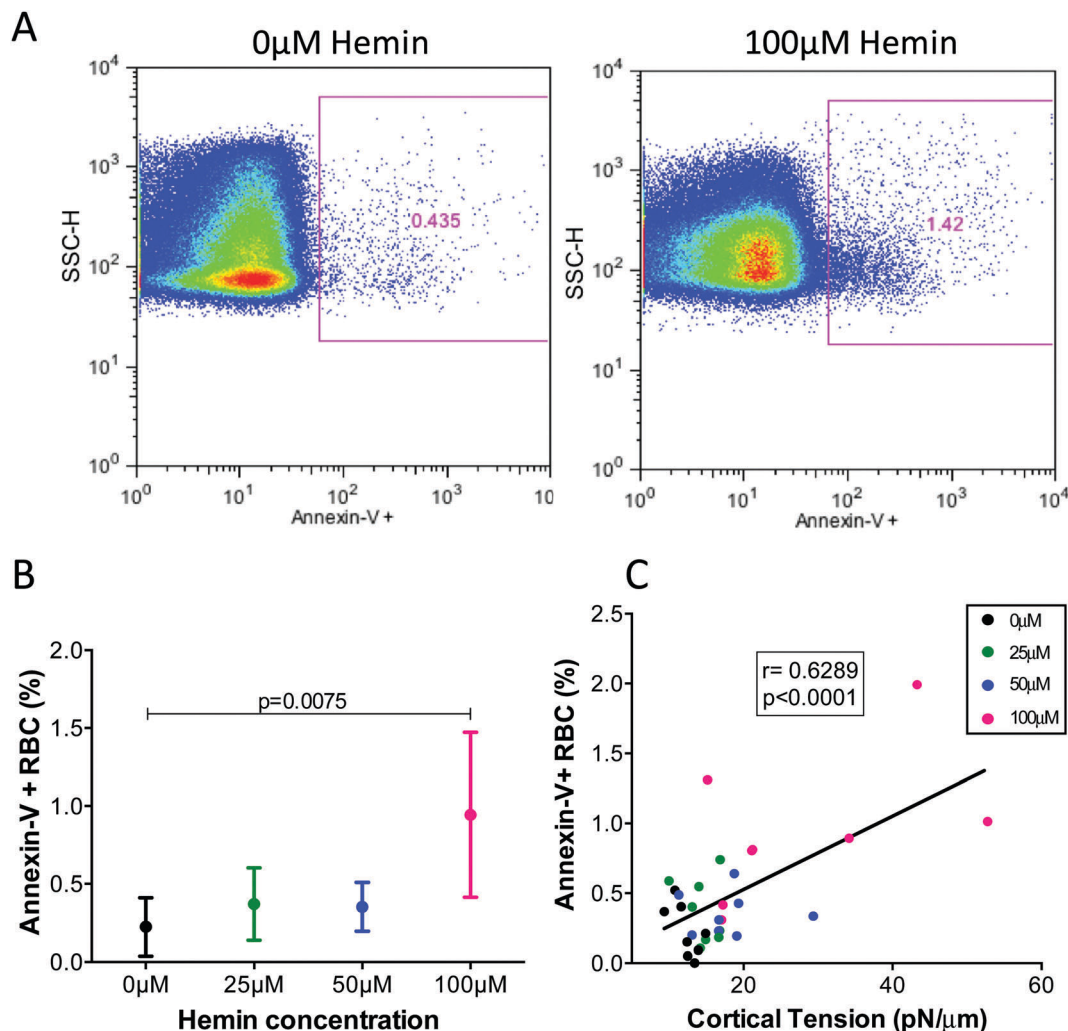


Fig. 4 Subpopulation analysis of RBC deformability shows pronounced loss in deformability. (A) The percent change in the deformability (increase in cortical tension) of the least deformable 10% of each RBC population relative to untreated control (Kruskal–Wallis ANOVA  $p < 0.0001$ ). (B) Distribution of the cortical tension for the 10% least deformable RBCs for each hemin concentration.



**Fig. 5** Hemin causes increased expression of Annexin-V on RBCs. (A) Representative flow cytometry scatter plots of the Annexin-V population for RBCs treated with 0 and 100  $\mu\text{M}$  of hemin. (B) There is a trend towards increasing Annexin-V staining with increasing hemin concentrations (ANOVA,  $p = 0.0004$ ), with the most obvious increase from 0  $\mu\text{M}$  was when RBCs were treated with 100  $\mu\text{M}$  hemin was statistically significant ( $p = 0.0075$ ). (C) We show a positive correlation of the mean cortical tension of hemin treated RBCs to the proportions of externalized PS as measured by Annexin-V expression (Pearson  $r = 0.6289$ ,  $p < 0.0001$ ).

externalization is punctuated in the range of 50  $\mu\text{M}$  and 100  $\mu\text{M}$  hemin (Fig. 5B). These results underscore the potential value for measurement of RBC deformability as a robust indicator of hemin-induced oxidative stress.

#### Measurable changes in deformability and erythrophagocytosis of bystander RBCs may be induced by hemolysis of parasitized cells

Hemolytic anemia caused by malaria is a serious health concern for children and pregnant women. This anemia typically arises from the sequestration and phagocytosis of both parasitized and bystander RBCs in the inter-endothelial cleft of the spleen. Erythrophagocytosis stems from the direct detection of externalized PS,<sup>50</sup> using Tim1, Tim4 and Stabilin-2<sup>51,52</sup> receptors or detection of immunoglobulin opsonization by Fc $\gamma$  macrophage receptors.<sup>53</sup> Over the past three decades, the monocyte monolayer assay (MMA) has proven to be a reliable indicator of hemolytic blood

transfusion.<sup>54,55</sup> We extended this established method to examine whether hemin-mediated oxidative stress influences erythrophagocytosis, we incubated washed RhD<sup>+</sup> RBCs with PBS buffer only (negative control), a range of hemin concentrations in PBS or with anti-RhD (positive control). These cells were overlaid on a monocyte monolayer assay (MMA) was used to measure the effect of hemin challenge of human RBC on immunologic recognition.<sup>56</sup> The monocyte index (MI) represents the number of erythrocytes phagocytosed per 100 monocytes. Compared to anti-RhD opsonized cells, with an MI of 67, hemin treatment induced a dose-dependent increase in erythrophagocytosis (Fig. 6A). In blood transfusion, MI values of  $\leq 5$ –6 indicate that donor cells carry a low risk of acute hemolytic reaction.<sup>57</sup> Consistent with the induction of oxidative stress, these cells were also more prone to hemolysis, when challenged by osmotic fragility assay (Fig. 6B). Together, these data suggest that hemolytic stress may precipitate erythrophagocytosis and promote malarial

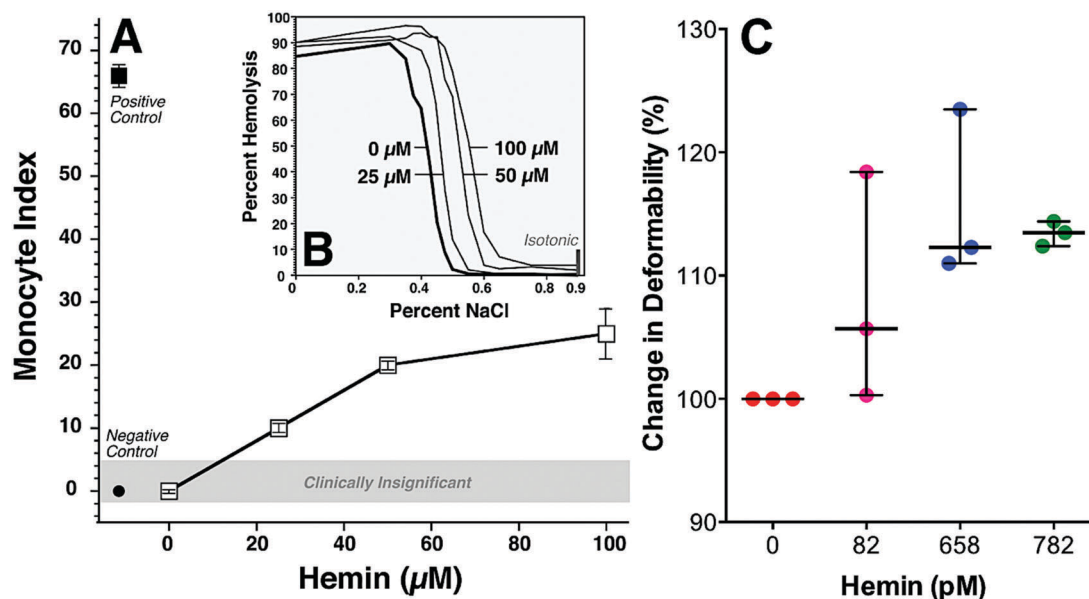


**Fig. 6** Effect of hemin treatment on immune recognition and RBC stability. (A) The number of adherent and phagocytosed control and opsonized RBCs were enumerated per 100 monocytes (monocyte index). There is significant increased recognition and phagocytosis of RBCs treated with increased concentrations of hemin, which (B) further correlates to the increased hemolysis observed in the osmotic fragility assay. (C) Deformability-based analysis represents a highly sensitive means to monitor the hemolytic bystander effect of RBCs that were exposed to malaria cell culture supernatant with known concentrations of hemin (median  $\pm$  interquartile range, Kruskal–Wallis,  $p < 0.0001$ ).

anemia. However, an important consideration is that RBC hemolysis may occur only infrequently and extracellular hemin may only circulate *in vivo* at very low concentration. To address this, we incubated RBCs in malaria culture supernatant prepared from 3 different *P. falciparum* 3D7 cultures (ranging 2–4% parasitemia) and measured both the free hemin concentration and change in RBC deformability within these cultures. These experiments revealed that changes in RBC deformability could be observed even at picomolar concentrations of hemin (Fig. 6C), making RBC deformability measurement potentially a highly sensitive measure of hemolytic stress.

## Discussion and conclusion

It has been previously established that the presence of one parasitized RBC in circulation indicates the loss of eight bystander RBC in falciparum malaria,<sup>58,59</sup> and 34 in vivax malaria.<sup>60</sup> This phenomenon could be partly explained by the increase in cell-free plasma heme and hemoglobin in severe malaria,<sup>61,62</sup> which contributes to rigidification of these cells due to cytoskeletal cross-linking<sup>5</sup> and lipid peroxidation<sup>6,7,63</sup> and their subsequent erythrophagocytosis by macrophages.<sup>9</sup> Such oxidative stressors have long been known to impact cell deformability<sup>64</sup> and our recent development of the multiplex fluidic plunger has provided the opportunity to sensitively measure changes in the deformability of multiple single RBCs.<sup>14</sup> Leveraging this new capability, we demonstrate that this device enables robust assessment of hemin-induced oxidative stress in RBCs.

During severe malarial anemia, RBC undergo eryptosis,<sup>47</sup> which is analogous to apoptosis for nucleated cells.<sup>65</sup> This process contributes to the emergence of reactive oxygen species

(ROS) and the membrane externalization of phosphatidylserine. While these two cytological changes represent compelling potential markers for disease severity, ROS metabolites are very short-lived and difficult to monitor *in vivo*<sup>10</sup> while analysis of PS externalization requires expert training, as well as sophisticated flow cytometry equipment along with reagents that require refrigerated storage. In contrast, we demonstrated that the MFP device detects long-lasting biophysical changes in RBCs resulting from hemolytic stress using an entirely mechanical process. Consequently, this technology could potentially be used at the point-of-care in low-resource environments to assist patient evaluation in severe malaria.<sup>66</sup>

The response of both malaria parasitized RBCs and bystander RBCs to hemolytic stress is garnering increasing attention as a method to assess disease severity,<sup>11–13</sup> as well as to monitor anti-malarial drug efficacy.<sup>14–16</sup> Changes in RBC deformability not only serves as a robust marker of hemolytic stress but is directly associated to malaria pathogenesis, owing to the enhanced splenic elimination of these cells<sup>67,68</sup> and its contribution to severe malaria. Furthermore, RBC rigidification may also contribute to death as both rigid parasitized and bystander cells may sequester within and obstruct the vasculature.<sup>69</sup> The MFP device provides an important opportunity to monitor the biophysical changes of RBCs at a single-cell resolution, providing valuable insight into both patient status and the underlying mechanisms for RBC sequestration and elimination in severe malaria.

## Acknowledgements

This work was supported by grants from the Canadian Institutes of Health Research and the Canadian Blood Services.

## References

- 1 WHO, World Malaria Report 2014. WHO, 2015. Available at: [http://www.who.int/malaria/publications/world\\_malaria\\_report\\_2014/en/](http://www.who.int/malaria/publications/world_malaria_report_2014/en/), accessed: 7th October 2015.
- 2 S. E. Francis, D. J. Sullivan and D. E. Goldberg, Hemoglobin Metabolism in the Malaria Parasite *Plasmodium falciparum*, *Annu. Rev. Microbiol.*, 1997, **51**, 97–123.
- 3 D. Schaer, P. Buehler, A. Alayash, J. Belcher and G. Vercellotti, Hemolysis and free hemoglobin revisited: exploring hemoglobin and heme scavengers as a novel class of therapeutic proteins, *Blood*, 2012, 1–24, DOI: 10.1182/blood-2012-11-451229.
- 4 F. F. Dutra, *et al.*, Hemolysis-induced lethality involves inflammasome activation by heme, *Proc. Natl. Acad. Sci. U. S. A.*, 2014, **111**, E4110–E4118.
- 5 L. M. Snyder, *et al.*, Effect of Hydrogen-Peroxide Exposure on Normal Human-Erythrocyte Deformability, Morphology, Surface Characteristics, and Spectrin-Hemoglobin Cross-Linking, *J. Clin. Invest.*, 1985, **76**, 1971–1977.
- 6 T. P. Flynn, D. W. Allen, G. J. Johnson and J. G. White, Oxidant damage of the lipids and proteins of the erythrocyte membranes in unstable hemoglobin disease. Evidence for the role of lipid peroxidation, *J. Clin. Invest.*, 1983, **71**, 1215–1223.
- 7 K. J. Davies and A. L. Goldberg, Oxygen radicals stimulate intracellular proteolysis and lipid peroxidation by independent mechanisms in erythrocytes, *J. Biol. Chem.*, 1987, **262**, 8220–8226.
- 8 A. J. Schroit, J. W. Madsen and Y. Tanaka, *In vivo* recognition and clearance of red blood cells containing phosphatidylserine in their plasma membranes, *J. Biol. Chem.*, 1985, **260**, 5131–5138.
- 9 L. T. Chen and L. Weiss, The role of the sinus wall in the passage of erythrocytes through the spleen, *Blood*, 1973, **41**, 529–537.
- 10 S. I. Dikalov and D. G. Harrison, Methods for detection of mitochondrial and cellular reactive oxygen species, *Antioxid. Redox Signaling*, 2014, **20**, 372–382.
- 11 S. Chien, S. Usami and J. F. Bertles, Abnormal Rheology of Oxygenated Blood in Sickle Cell Anemia, *J. Clin. Invest.*, 1970, **49**, 623.
- 12 N. Mohandas, W. M. Phillips and M. Bessis, Red blood cell deformability and hemolytic anemias, *Semin. Hematol.*, 1979, **16**, 95–114.
- 13 E. Shinar and E. A. Rachmilewitz, Oxidative denaturation of red blood cells in thalassemia, *Semin. Hematol.*, 1990, **27**, 70–82.
- 14 M.-E. Myrand-Lapierre, *et al.*, Multiplexed fluidic plunger mechanism for the measurement of red blood cell deformability, *Lab Chip*, 2015, **15**, 159–167.
- 15 A. T. Santoso, *et al.*, Microfluidic cell-phoresis enabling high-throughput analysis of red blood cell deformability and biophysical screening of antimalarial drugs, *Lab Chip*, 2015, **15**, 4451–4460.
- 16 X. Deng, *et al.*, Reduced deformability of parasitized red blood cells as a biomarker for anti-malarial drug efficacy, *Malar. J.*, 2015, **14**, 428.
- 17 M. Bessis, N. Mohandas and C. Feo, Automated ektacytometry: a new method of measuring red cell deformability and red cell indices, *Blood Cells*, 1980, **6**, 315.
- 18 M. R. Clark, N. Mohandas and S. B. Shoheit, Osmotic gradient ektacytometry: comprehensive characterization of red cell volume and surface maintenance, *Blood*, 1983, **61**, 899–910.
- 19 O. K. Baskurt, *et al.*, Comparison of three commercially available ektacytometers with different shearing geometries, *Biorheology*, 2009, **46**, 251–264.
- 20 G. J. Streekstra, J. G. G. Dobbe and A. G. Hoekstra, Quantification of the fraction poorly deformable red blood cells using ektacytometry, *Opt. Express*, 2010, **18**, 14173–14182.
- 21 M. D. Scott, *et al.*, Qinghaosu-Mediated Oxidation in Normal and Abnormal Erythrocytes, *J. Lab. Clin. Med.*, 1989, **114**, 401–406.
- 22 F. Kuypers, M. Scott, M. Schott, B. Lubin and D. Chiu, Use of ektacytometry to determine red cell susceptibility to oxidative stress, *J. Lab. Clin. Med.*, 1990, **116**, 535–545.
- 23 K. Lopez-Shirley, F. Zhang, D. Gosser, M. Scott and S. R. Meshnick, Antimalarial quinones: redox potential dependence of methemoglobin formation and heme release in erythrocytes, *J. Lab. Clin. Med.*, 1994, **123**, 126–130.
- 24 M. Dao, C. T. Lim and S. Suresh, Mechanics of the human red blood cell deformed by optical tweezers, *J. Mech. Phys. Solids*, 2003, **51**, 2259–2280.
- 25 T. Herricks, M. Antia and P. K. Rathod, Deformability limits of *Plasmodium falciparum*-infected red blood cells, *Cell. Microbiol.*, 2009, **11**, 1340–1353.
- 26 J. Kwan, Q. Guo, D. Kyliuk-Price, H. Ma and M. Scott, Microfluidic analysis of cellular deformability of normal and oxidatively damaged red blood cells, *Am. J. Hematol.*, 2013, **88**, 682–689.
- 27 Y. J. Kang, Y.-R. Ha and S.-J. Lee, High-Throughput and Label-Free Blood-on-a-Chip for Malaria Diagnosis, *Anal. Chem.*, 2016, **88**, 2912–2922.
- 28 S. S. Lee, Y. Yim, K. H. Ahn and S. J. Lee, Extensional flow-based assessment of red blood cell deformability using hyperbolic converging microchannel, *Biomed. Microdevices*, 2009, **11**, 1021–1027.
- 29 A. M. Forsyth, J. Wan, W. D. Ristenpart and H. A. Stone, The dynamic behavior of chemically ‘stiffened’ red blood cells in microchannel flows, *Microvasc. Res.*, 2010, **80**, 37–43.
- 30 A. Bransky, N. Korin, Y. Nemirovski and U. Dinnar, Correlation between erythrocytes deformability and size: a study using a microchannel based cell analyzer, *Microvasc. Res.*, 2007, **73**, 7–13.
- 31 Q. Guo, S. J. Reiling, P. Rohrbach and H. Ma, Microfluidic biomechanical assay for red blood cells parasitized by *Plasmodium falciparum*, *Lab Chip*, 2012, **12**, 1143–1150.
- 32 H. Bow, *et al.*, A microfabricated deformability-based flow cytometer with application to malaria, *Lab Chip*, 2011, **11**, 1065.
- 33 H. Ito, *et al.*, Mechanical diagnosis of human erythrocytes by ultra-high speed manipulation unraveled critical time window for global cytoskeletal remodeling, *Sci. Rep.*, 2017, **7**, 43134.



- 34 J. Amer, A. Goldfarb and E. Fibach, Flow cytometric measurement of reactive oxygen species production by normal and thalassaemic red blood cells, *Eur. J. Haematol.*, 2003, **70**, 84–90.
- 35 G. C. Rampersad, *et al.*, Chemical compounds that target thiol-disulfide groups on mononuclear phagocytes inhibit immune mediated phagocytosis of red blood cells, *Transfusion*, 2005, **45**, 384–393.
- 36 D. R. Branch, M. T. Gallagher, A. P. Mison, A. L. Sy Siok Hian and L. D. Petz, *In vitro* determination of red cell alloantibody significance using an assay of monocyte-macrophage interaction with sensitized erythrocytes, *Br. J. Haematol.*, 1984, **56**, 19–29.
- 37 V. Karamatic Crew, *et al.*, Two MER2-negative individuals with the same novel CD151 mutation and evidence for clinical significance of anti-MER2, *Transfusion*, 2008, **48**, 1912–1916.
- 38 M. T. Gallagher, D. R. Branch, A. Mison and L. D. Petz, Evaluation of reticuloendothelial function in autoimmune hemolytic anemia using an *in vitro* assay of monocyte-macrophage interaction with erythrocytes, *Exp. Hematol.*, 1983, **11**, 82–89.
- 39 L. Li, G. T. Noumsi, Y. Y. E. Kwok, J. M. Moulds and M. D. Scott, Inhibition of phagocytic recognition of anti-D opsonized Rh D+ RBC by polymer-mediated immunocamouflage, *Am. J. Hematol.*, 2015, **90**, 1165–1170.
- 40 M. D. Scott, *et al.*, Structural and functional consequences of antigenic modulation of red blood cells with methoxypoly(ethylene glycol), *Blood*, 1999, **93**, 2121–2127.
- 41 M. D. Scott, K. L. Murad, F. Koumpouras, M. Talbot and J. W. Eaton, Chemical camouflage of antigenic determinants: Stealth erythrocytes, *Proc. Natl. Acad. Sci. U. S. A.*, 1997, **94**, 7566–7571.
- 42 A. Radfar, *et al.*, Synchronous culture of *Plasmodium falciparum* at high parasitemia levels, *Nat. Protoc.*, 2009, **4**, 1828–1844.
- 43 H. Y. Ho, *et al.*, Enhanced oxidative stress and accelerated cellular senescence in glucose-6-phosphate dehydrogenase (G6PD)-deficient human fibroblasts, *Free Radical Biol. Med.*, 2000, **29**, 156–169.
- 44 K. Matthews, *et al.*, Microfluidic deformability analysis of the red cell storage lesion, *J. Biomech.*, 2015, **48**, 4065–4072.
- 45 Q. Guo, S. Park and H. Ma, Microfluidic micropipette aspiration for measuring the deformability of single cells, *Lab Chip*, 2012, **12**, 2687–2695.
- 46 Q. Guo, *et al.*, Microfluidic analysis of red blood cell deformability, *J. Biomech.*, 2014, **47**, 1767–1776.
- 47 F. Lang, K. S. Lang, P. A. Lang, S. M. Huber and T. Wieder, Mechanisms and significance of eryptosis, *Antioxid. Redox Signaling*, 2006, **8**, 1183–1192.
- 48 S. Eda and I. W. Sherman, Cytoadherence of malaria-infected red blood cells involves exposure of phosphatidylserine, *Cell. Physiol. Biochem. Int. J. Exp. Cell. Physiol. Biochem. Pharmacol.*, 2002, **12**, 373–384.
- 49 C. Fernandez-Arias, *et al.*, Anti-Self Phosphatidylserine Antibodies Recognize Uninfected Erythrocytes Promoting Malarial Anemia, *Cell Host Microbe*, 2016, **19**, 194–203.
- 50 K. De Jong, *et al.*, Short survival of phosphatidylserine-exposing red blood cells in murine sickle cell anemia, *Blood*, 2001, **98**, 1577–1584.
- 51 N. Kobayashi, *et al.*, TIM-1 and TIM-4 glycoproteins bind phosphatidylserine and mediate uptake of apoptotic cells, *Immunity*, 2007, **27**, 927–940.
- 52 S.-Y. Park, *et al.*, Rapid cell corpse clearance by stabilin-2, a membrane phosphatidylserine receptor, *Cell Death Differ.*, 2008, **15**, 192–201.
- 53 T. Berney, *et al.*, Murine autoimmune hemolytic anemia resulting from Fc gamma receptor-mediated erythrophagocytosis: protection by erythropoietin but not by interleukin-3, and aggravation by granulocyte-macrophage colony-stimulating factor, *Blood*, 1992, **79**, 2960–2964.
- 54 S. J. Nance, P. Arndt and G. Garratty, Predicting the clinical significance of red cell alloantibodies using a monocyte monolayer assay, *Transfusion*, 1987, **27**, 449–452.
- 55 P. A. Arndt and G. Garratty, A retrospective analysis of the value of monocyte monolayer assay results for predicting the clinical significance of blood group alloantibodies, *Transfusion*, 2004, **44**, 1273–1281.
- 56 D. L. Kyliuk-Price, L. Li and M. D. Scott, Comparative efficacy of blood cell immunocamouflage by membrane grafting of methoxypoly(ethylene glycol) and polyethyloxazoline, *Biomaterials*, 2014, **35**, 412–422.
- 57 T. N. Tong, *et al.*, Optimal conditions for the performance of a monocyte monolayer assay, *Transfusion (Paris)*, 2016, **56**, 2680–2690.
- 58 G. N. Jakeman, A. Saul, W. L. Hogarth and W. E. Collins, Anaemia of acute malaria infections in non-immune patients primarily results from destruction of uninfected erythrocytes, *Parasitology*, 1999, **119**(Pt 2), 127–133.
- 59 R. N. Price, *et al.*, Factors contributing to anemia after uncomplicated falciparum malaria, *Am. J. Trop. Med. Hyg.*, 2001, **65**, 614–622.
- 60 W. E. Collins, G. M. Jeffery and J. M. Roberts, A retrospective examination of anemia during infection of humans with *Plasmodium vivax*, *Am. J. Trop. Med. Hyg.*, 2003, **68**, 410–412.
- 61 B. B. Andrade, *et al.*, Heme impairs prostaglandin E2 and TGF-beta production by human mononuclear cells via Cu/Zn superoxide dismutase: insight into the pathogenesis of severe malaria, *J. Immunol.*, 2010, **185**, 1196–1204.
- 62 T. W. Yeo, *et al.*, Relationship of cell-free hemoglobin to impaired endothelial nitric oxide bioavailability and perfusion in severe falciparum malaria, *J. Infect. Dis.*, 2009, **200**, 1522–1529.
- 63 M. D. Scott and J. W. Eaton, Thalassaemic erythrocytes: cellular suicide arising from iron and glutathione-dependent oxidation reactions?, *Br. J. Haematol.*, 1995, **91**, 811–819.
- 64 S. Chien, Red cell deformability and its relevance to blood flow, *Annu. Rev. Physiol.*, 1987, **49**, 177–192.
- 65 *Point-of-Care Diagnostics on a Chip*, ed. D. Issadore and R. M. Westervelt, Springer, Berlin, Heidelberg, 2013, DOI: 10.1007/978-3-642-29268-2.

- 66 P. R. R. Totino, C. T. Daniel-Ribeiro and M. de F. Ferrreira-da-Cruz, Evidencing the Role of Erythrocytic Apoptosis in Malarial Anemia, *Front. Cell. Infect. Microbiol.*, 2016, **6**, 176.
- 67 G. B. Nash, Red cell mechanics: what changes are needed to adversely affect in vivo circulation, *Biorheology*, 1991, **28**, 231–239.
- 68 G. Deplaine, *et al.*, The sensing of poorly deformable red blood cells by the human spleen can be mimicked in vitro, *Blood*, 2011, **117**, e88–e95.
- 69 N. J. White, G. D. H. Turner, N. P. J. Day and A. M. Dondorp, Lethal malaria: Marchiafava and Bignami were right, *J. Infect. Dis.*, 2013, **208**, 192–198.